Volume 23
Number 10
21 May 2023
Pages 2359–2488

Lab on a Chip

Devices and applications at the micro- and nanoscale

rsc.li/loc

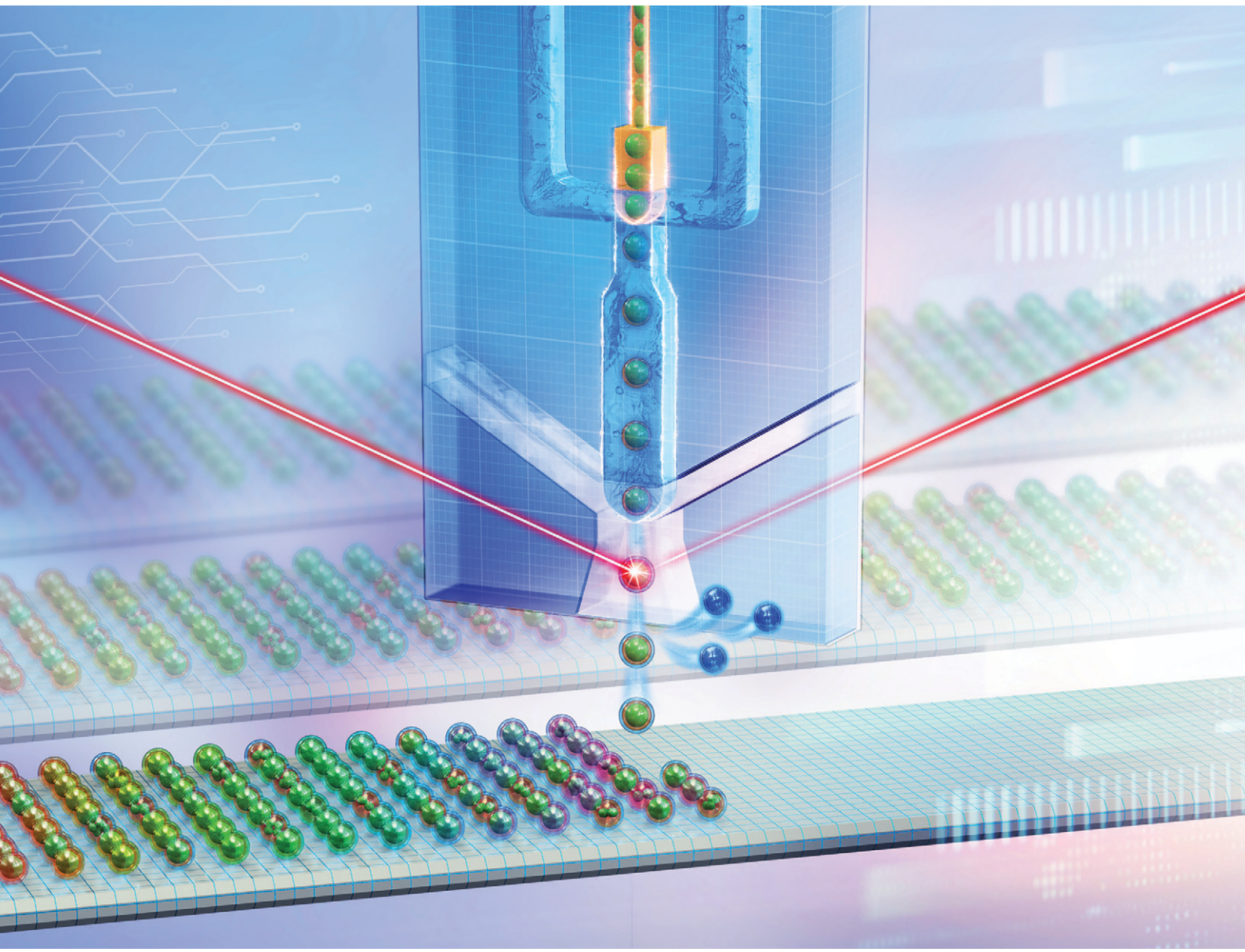

ISSN 1473-0197

ROYAL SOCIETY OF CHEMISTRY

PAPER

Pengfei Zhang, Adam R. Abate *et al.*
Flow cytometric printing of double emulsions into open droplet arrays

Lab on a Chip

PAPER

View Article Online
View Journal | View Issue

Cite this: *Lab Chip*, 2023, **23**, 2371

Flow cytometric printing of double emulsions into open droplet arrays†

Pengfei Zhang, [ab] Linfeng Xu,[b] Huawei Chen [a] and Adam R. Abate *[bc]

Received 22nd February 2023,
Accepted 11th April 2023

DOI: 10.1039/d3lc00151b

rsc.li/loc

Delivery of double emulsions in air is crucial for their applications in mass spectrometry, bioanalytics, and material synthesis. However, while methods have been developed to generate double emulsions in air, controlled printing of double emulsion droplets has not been achieved yet. In this paper, we present an approach for in-air printing of double emulsions on demand. Our approach pre-encapsulates reagents in an emulsion that is reinjected into the device, and generates double emulsions in a microfluidic printhead with spatially patterned wettability. Our device allows sorting of ejected double emulsion droplets in real-time, allowing deterministic printing of each droplet to be selected with the desired inner cores. Our method provides a general platform for building printed double emulsion droplet arrays of defined composition at scale.

Introduction

Double emulsions are complex colloidal systems and consist of single or multiple liquid inner cores that are separated from a carrier fluid by a layer of immiscible liquid shell.[1–3] The core–shell structure of the double emulsions allows manipulation of the compositions *via* encapsulating the desired materials in the inner cores or tuning liquids of the shells.[4,5] This property affords synthesis of various types of particles and capsules, which have found diverse applications in areas of food, cosmetics, pharmaceutics, and biology, such as the production of low-calorie food, synthesis of chemicals, controlled delivery and release of drugs, and directed evolution of enzymes and proteins.[6–11]

Microfluidics has emerged as an effective platform to make monodispersed double emulsions, and exhibits unmatched controllability and flexibility by tuning of the wettability and dimensions of microfluidic channels.[12–16] In general, the generation of double emulsions in a microfluidic device is mainly in liquid phase; liquid carrier flow provides a steady shear stress and can disperse continuous liquids to form double emulsions in a controllable manner.[12,14] While it is more challenging to utilize air flow to make double emulsions, there are many cases that controllable delivery of double emulsions in air are valuable.[17–22] For instance, ejecting of double emulsions with unstable compounds encapsulated in the inner cores can address their targeted delivery in air, precision ejection of double emulsion droplets allows their interfacing with the activated component in a mass spectrometer, and printing of double emulsion droplets onto analytical substrates allows high-throughput screening of biological assays.

Methods for generation of double emulsions in air mainly rely on two types of mechanism, one utilizing a gas stream to shear off the continuous liquid phase and the other one based on forces arising from an electric filed.[23–27] Because gases have a much lower viscosity compared with that of a liquid phase, there is a need of high pressure of gas flow to generate enough shear stress such that droplets can be formed.[23,26,27] In this case, however, droplet formation works in the jetting regime, typically yielding a high generation speed, which is difficult to be utilized subsequently, such as interfacing with mass spectrometry. Electrospray technique utilizes electrohydrodynamic forces to generate coaxial jets of immiscible liquids through two concentric tubes or microfluidic channels, with the inner one containing an aqueous solution and the outer one containing oil.[24,25] The compound jet can be emitted under the actuation of electrical signals to generate double emulsions. Although the generation speed is low (tens to hundreds of Hz), without manipulation of ejected droplets, the ejection is not on-demand, and thus it is not suitable to be utilized for applications like printing. To enable controllable generation of double emulsions in air with utility for printing, an optimal method would be developed with a capability of precise manipulation of droplets during generation and ejection.

[a] *School of Mechanical Engineering and Automation, Beihang University, Beijing, China*
[b] *Department of Bioengineering and Therapeutic Sciences, University of California, San Francisco, San Francisco, CA, USA. E-mail: adam@abatelab.org*
[c] *California Institute for Quantitative Biosciences, University of California, San Francisco, San Francisco, CA, USA*

† Electronic supplementary information (ESI) available. See DOI: **https://doi.org/10.1039/d3lc00151b**

In this paper, we describe an approach that is capable of deterministically printing double emulsion droplets onto open substrates. The core feature of this approach is the construction of a flow-focusing geometry with spatial wettability patterns in a microfluidic printhead integrated with an in-air droplet sorter. Wetting treatment in microfluidic channels enables controlled generation of the double emulsions, which are subsequently ejected by shear stress exerted from focused air streams. Ejected double emulsion droplets are interrogated by a droplet sorter, and on-demand printing is achieved by selectively sorting. We demonstrate this approach by printing double emulsion droplet arrays through selecting ones with desired fluorescent inner cores. Our approach provides a means for analysis of double emulsions by deterministic printing.

Results and discussion

Generation of double emulsions in air relies on one external force exerted on the fluids at the emission nozzle such that the droplets can be formed and ejected.[23–25] Co-flowing of a high-pressure gas stream with two concentric tubes, with fluids flowing within, results in ejection of double emulsions; however, the strong shear stress makes a very high

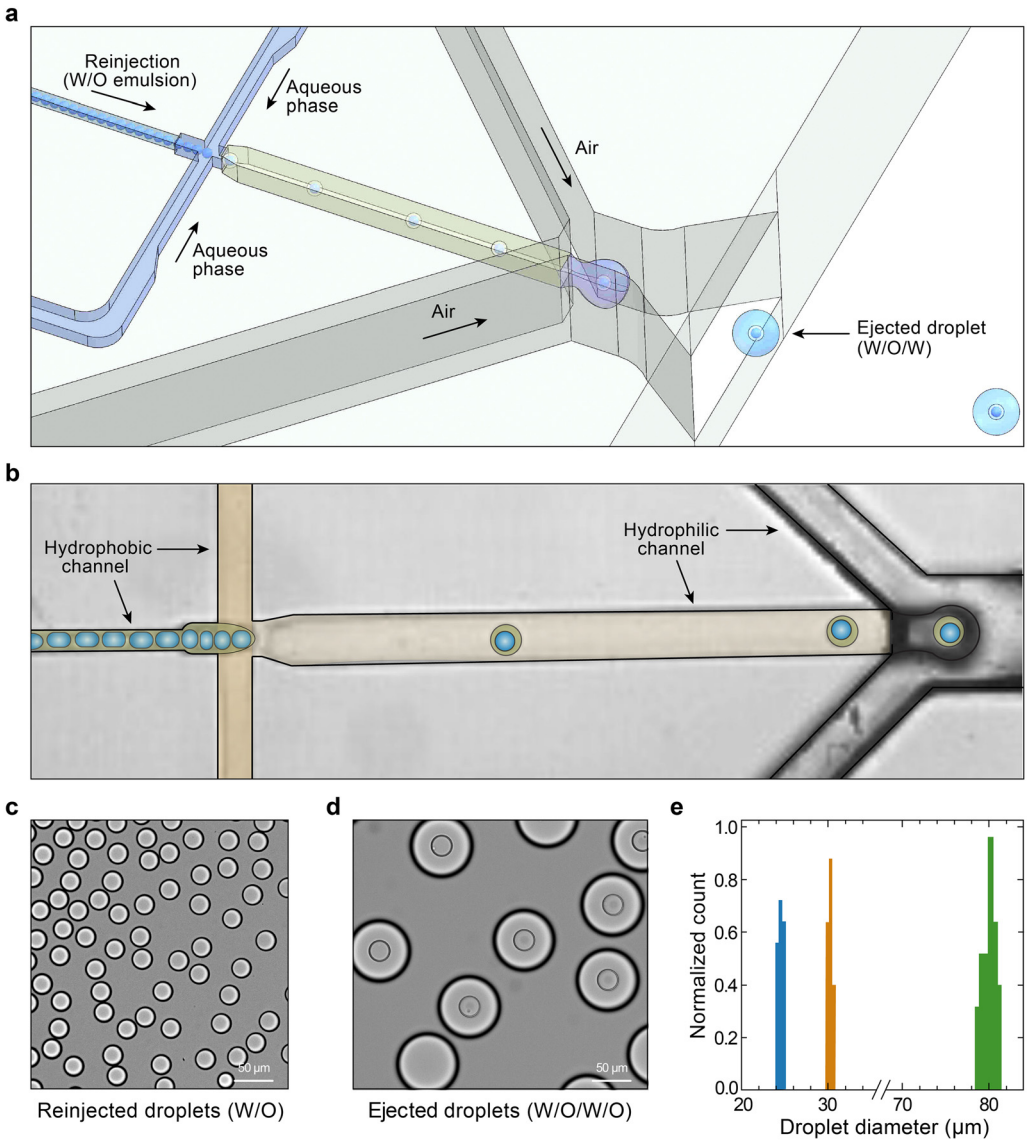

Fig. 1 Design and operation of the microfluidic device to generate double emulsions in air. (a) Schematic of the microfluidic device. Reinjected water-in-oil (W/O) single emulsions are dispersed by an aqueous phase at the flow-focusing junction, resulting in generation of water-in-oil-in-water (W/O/W) double emulsions, which are subsequently dispersed and ejected by a co-flow of two air streams. (b) Design of the wettability patterns in microfluidic channels, where hydrophobicity is maintained upstream the flow-focusing junction, and the channel downstream the flow-focusing junction is made with hydrophilicity to prevent wetting of the double emulsion droplets. (c) Image of reinjected W/O single emulsion droplets. (d) Image of triple emulsion droplets obtained by collecting ejected W/O/W double emulsion droplets in the oil phase. The size of the different phases in the triple emulsion droplets is shown in (e).

generation speed. In addition, double emulsion droplets and their inner cores are simultaneously formed, leaving no space for manipulation. We would like to generate double emulsions in a slower and controllable speed, and generate the inner cores before ejection such that we can manipulate their compositions. To achieve this, we reinject a water-in-oil (W/O) single emulsion and produce water-in-oil-in-water (W/O/W) double emulsions in the device through standard flow-focusing of continuous single emulsions and outer disperse aqueous phase (Fig. 1a).

To prohibit the wetting of droplets, we construct a wettability pattern in microfluidic channels, hydrophobicity for W/O emulsions and hydrophilicity for W/O/W double emulsions (Fig. 1b). To enable a controllable ejection with a lower speed, we need to decrease the pressure needed to shear off double emulsions. Instead of flowing air stream in an open space, we make two air streams flow in constrained channels and focus them on the emission nozzle; this design allows dripping generation of double emulsion droplets in air with a controllable speed. Based on these properties, our device allows a stable ejection of monodispersed W/O/W double emulsion droplets with uniform sizes (Fig. 1c–e). The resultant droplets consist of the double emulsions encapsulated within carrier aqueous droplets in air moving at a nearly constant velocity. Different from previous studies, we eject W/O/W droplets but not W/O droplets in air; thus, when collected in oil, these droplets generate triple emulsions (Fig. 1d), which allow us to characterize their sizes and uniformity. Ejected double emulsion droplets are pretty uniform with a polydispersity index of ~0.01%; ejected triple emulsion droplets show a size variation of ~102 μm to ~76 μm with varying air pressure in the tested device (Fig. S1†).

To make double emulsions in a microfluidic device, one crucial step is to construct wettability patterns.[15,28] To construct wettability patterns in the microfluidic device for double emulsion generation and encapsulation, we use oxygen plasma treatment.[29] During treatment, all injection holes are covered and only the ejection nozzle is left open, allowing ionized oxygen species to diffuse into the channel. To ensure the channel downstream the flow-focusing junction with hydrophilicity for stable generation of double emulsions, we treat the device with oxygen plasma for 3 min. However, such a long-time treatment makes the channel around the nozzle with a very high hydrophilicity, which results in the wetting of liquids (Fig. 2a, upper). To obtain a wettability pattern enabling stable double emulsion ejection, we utilize baking of PDMS to controllably recover the hydrophobicity of microfluidic channels after oxygen plasma treatment.[30] The bake time must be controlled to obtain an optimal wettability in the first junction to encapsulate the single emulsions in double emulsions while also allowing the formation of water droplets in air in the second junction. A treatment that is too short leaves the entire device hydrophilic, interfering with water droplet formation in the air channel (Fig. 2a, upper), while a treatment that is too long results in a hydrophobic first junction, preventing the formation of the double emulsions (Fig. 2a, lower). By tuning oxygen plasma and post-bake times, we find that stable operation (Fig. 2a, middle, and Movie S1†) of both junctions occurs for contact angles between 35 and 83 degrees (Fig. 2b).

Control of the number of the inner cores in ejected double emulsion droplets are important if they are utilized to synthesize multimaterial particles and study cell–cell interactions or controlled micro-reactions.[31–33] Previous methods mainly generate and eject double emulsion droplets simultaneously, with poor control over the inner cores. Our device forms double emulsions before the ejection and thus, the inner cores can be precisely controlled. This can be achieved through holding the inner single emulsion flow rate constant while varying the outer aqueous phase flow rate. To

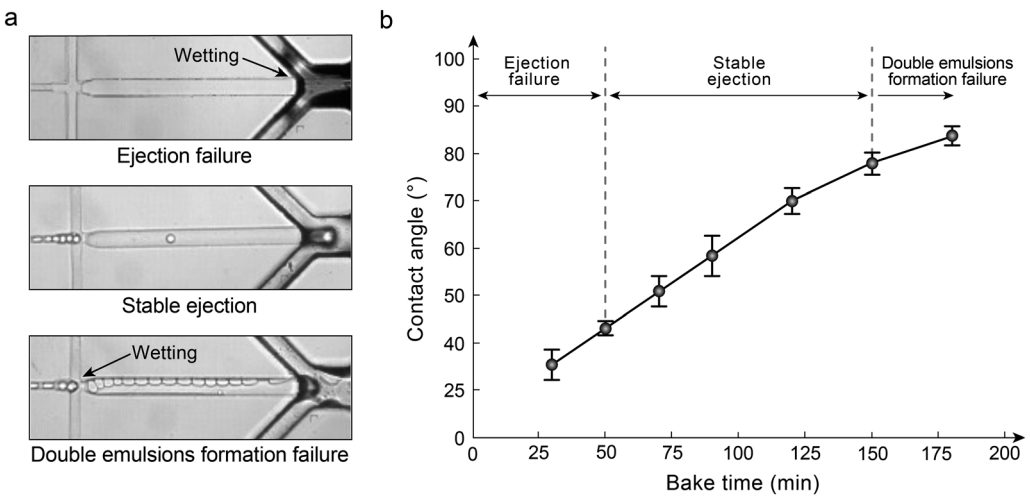

Fig. 2 Spatial wettability patterns enable stable generation and ejection of double emulsions. (a) Images showing three conditions of double emulsion formation and ejection in the microfluidic device with different wettability patterns. (b) The corresponding intrinsic contact angle in the microfluidic channel for the three ejection conditions shown in (a). Stable generation and ejection of double emulsions occur within a contact angle range of ~35° to 83°.

illustrate this, we set the flow rate of single emulsion at 10 μL h^{-1} and decrease the flow rate of aqueous phase starting from ~300 μL h^{-1}, at which stable one-core double emulsion droplets are formed. We observe the number of inner cores gradually increases with aqueous phase flow rate decrease (Fig. 3a and b and Movie S2†). When the aqueous phase flow rate is too low (below ~50 μL h^{-1}), too many cores generate a big double emulsion droplet, making it have contact with the microfluidic channel wall and leading to the device being broken-down after a short running time. The double emulsions are then encapsulated into the carrier phase droplets in air and can be captured into oil or aqueous phases. If captured into oil with a surfactant, the carrier droplet remains, yielding W/O/W/O triple emulsions (Fig. 3c). If captured into the aqueous phase, the carrier droplets merge with the collection fluid, leaving only W/O/W double emulsions (Fig. 3d). If double emulsions are generated with a mixture of two types of single emulsions, two types of double emulsion droplets are formed (Fig. S2†).

Although the double emulsion ejection with dripping allows precise manipulation of the generation speed, it stills works in a continuous manner, making it impossible to turn on and off the droplet generation rapidly. Printing of the double emulsions requires the droplets to be delivered on demand. To enable this, we implement a droplet sorter into the droplet generation device.[34] Our printing device thus can direct droplets onto any desired substrate, and allows for precise printing of double emulsions in open droplet arrays (Movie S3†). To demonstrate this, we create an emulsion of fluorescein solution and introduce it into the device. The droplets are encapsulated in double emulsions and then sorted for printing (Fig. 4a). Since the incoming fluorescein droplet rate is lower than the carrier droplet rate, most droplets are empty, with only a fraction containing fluorescent double emulsions (Fig. 4b, left). By instructing the sorter to only select droplets containing fluorescein, we achieve a pure population (Fig. 4b, middle) with a sorting accuracy of >99% (Fig. 4b, right). To demonstrate printing of double emulsions onto a solid substrate, we replace the oil collection fluid with a glass plate coated with a thin PDMS layer, first printing empty carrier droplets (Fig. 4c), and then carrier droplets containing one fluorescein double emulsion (Fig. 4d). The droplets evaporate within seconds of printing, leaving behind a fluorescent coffee-ring pattern when the fluorescein droplets are included.

Conclusions

We present a microfluidic approach to deterministically print double emulsion droplets in air. Our device achieves control over the generation of double emulsions by reinjecting single emulsions in a microfluidic device with spatial wettability patterns. With the integrated droplet sorter, the device can read and sort ejected double emulsion droplets. Since the composition in the inner core can be precisely controlled, as we have demonstrated, our method allows printing of diverse

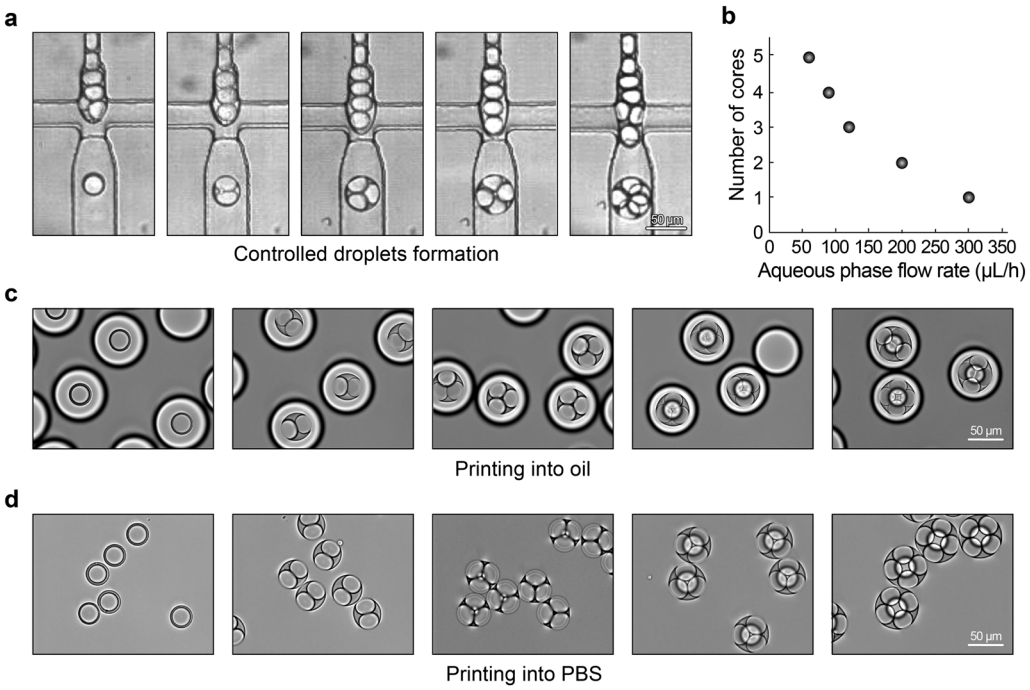

Fig. 3 Controlled multiple emulsion droplets formation and ejection. (a) Images of double emulsions with controlled inner cores by tuning flow rate. (b) Plot of the number of inner cores as a function of carrier aqueous flow rates. The reinjection flow rate is 10 μL h^{-1}. (c) Images of ejected double emulsion droplets printed in oil, showing triple emulsions with controlled inner cores. (d) Images of ejected double emulsion droplets printed in PBS, showing double emulsions with controlled inner cores. Empty droplets are merged into PBS allowing uniform double emulsions without empty drops.

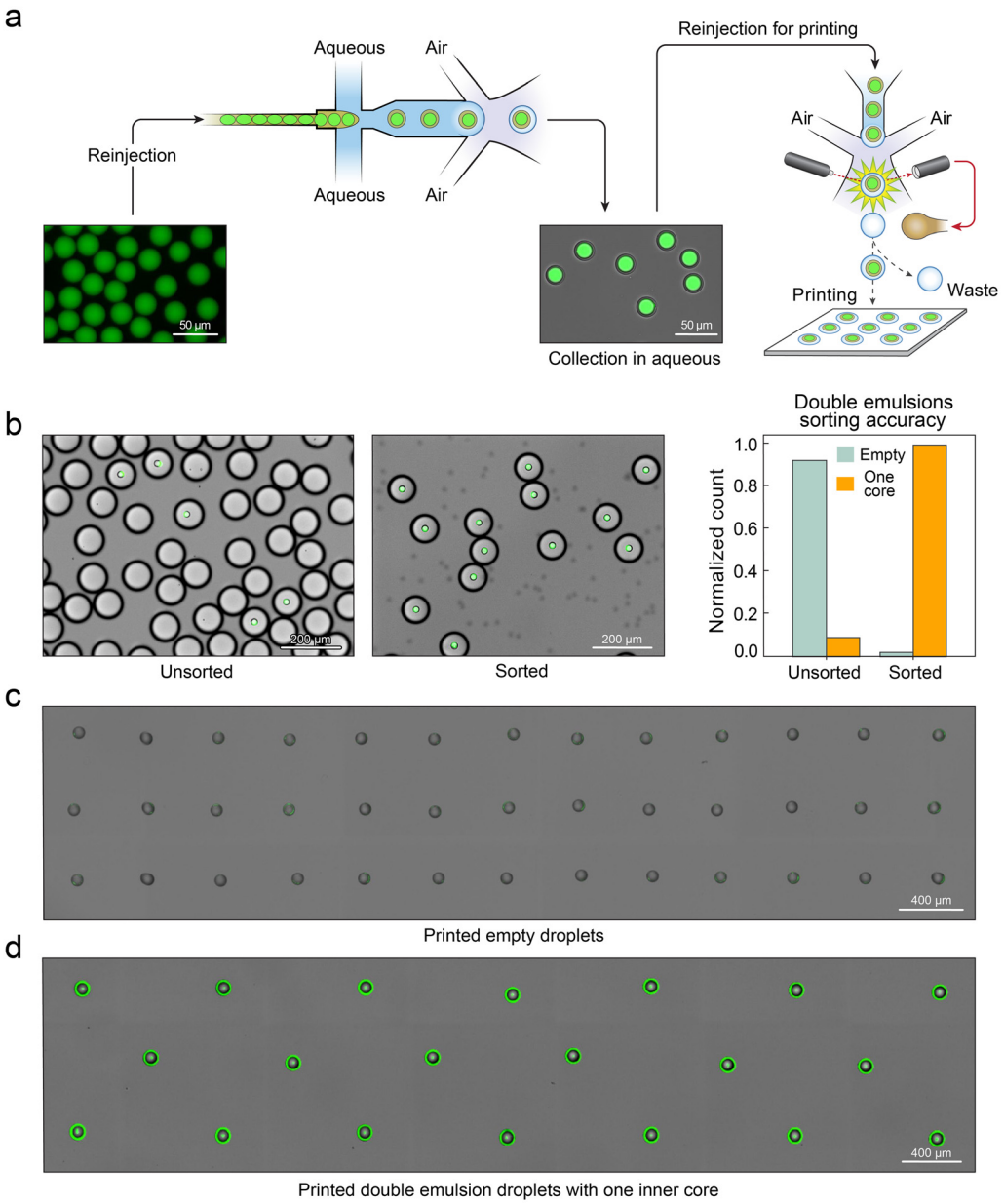

Fig. 4 On-demand printing of double emulsions in air. (a) Schematic of the printing process showing that single emulsion droplets are reinjected into the microfluidic print head, in which W/O/W double emulsions are generated at the first junction with carrier aqueous phase. Formed double emulsions are subsequently dispersed and ejected by focused air streams, followed by sorting for deterministic printing onto open substrates to construct droplet arrays. (b) Images of droplets without sorting (left) and with sorting (middle). Column plot showing sorting accuracy of the printing is beyond 99% (right). (c) Image of printed empty droplets array. (d) Image of printed double emulsion droplets array. Printed droplets show fluorescent green rings and inner dots, formed by the fluorescent inner cores after impacting onto the printing substrate.

droplet arrays. If reinjected emulsions are with combinatorial inner cores, multimaterial printing can be achieved by selective sorting. In addition, biological assays in droplets can be performed before the reinjection, and printing of these onto analytical substrates should enable high-throughput analysis. Because our device is made with standard lithography, it holds the potential for scale-up fabrication. The microfluidic chip is a device miniaturized at the millimeter scale, and thus it can be easily integrated in other instruments like mass spectrometers. Our approach extends the utility of double emulsions *via* printing and should find numerous valuable applications in high throughput biology and chemical screening.

Experimental section

Device fabrication

Microfluidic devices were fabricated using standard soft lithography from poly(dimethylsiloxane) (PDMS, RTV 615, Momentive, Waterford, NY, USA). Two types of microfluidic

devices were fabricated in this study: a flow-focusing device to generate water-in-oil single emulsion droplets, and a print head with stable double emulsion droplets ejection and integrated with sorting and printing modules. Masters with SU-8 structures were first fabricated on a 3 inch silicon wafer from photoresist (SU8, MicroChem, Westborough, MA, USA) using photolithography. Then, precured PDMS with a prepolymer and curing agent at a ratio of 10 : 1 was cast on the masters. After degassing in a vacuum chamber, and baking in an oven at 65 °C for 24 h, PDMS slabs were obtained by extraction from the masters. The holes in the PDMS slabs were punched by a 0.75 mm biopsy core. Structured PDMS was bonded onto a glass slide (water-in-oil droplet generator) or two PDMS slabs were bonded together (print head) with precise alignment to form the 3D structure after oxygen plasma treatment (Technics Plasma etcher). Devices were then baked in an oven at 65 °C for 2 days to render the channel hydrophobic. For the water-in-oil droplet generator, Aquapel was utilized to treat the microfluidic channels, while for the print head, wettability patterns were obtained by methods as follows.

Wettability patterning

The spatially-controlled plasma oxidation method was employed to create wettability patterns for a double emulsion droplets printer. Specifically, after a 2 day bake in an oven to fully recover the hydrophobicity of the microfluidic device, it was treated with oxygen plasma for 3 min. During this treatment, all punched holes were covered with tape. The treated devices were then baked in an oven at 85 °C for a certain time, partially recovering the hydrophobicity of the microfluidic channel to a range that enables double emulsion formation in the channel while allowing for double emulsion droplet ejection at the nozzle.

Double emulsion droplets formation and ejection

For the droplet formation system, the injection or reinjection of liquid phases or emulsions was controlled using syringe pumps (New Era, Farmingdale, NY). The airflow was manipulated by airflow controllers (900×, Control Air Inc., NH) which were controlled by a custom-made LabView interface. To form water-in-oil droplets, the aqueous phase was supplemented with 4% (v/v) Tween 20, 4% (w/v) PEG 4 k, and the oil phase was supplemented with 2% Weitz surfactant in HFE oil. To form double emulsion droplets, the outer aqueous phase was supplemented with 4% (v/v) Tween 20, 8% (w/v) PEG 4 k, and 1% Pluronic F-68. Droplet formation and ejection were monitored with a high-speed camera (Phantom Miro M-310, Vision Research). To characterize the ejected droplets, droplets were ejected into an oil phase (Novec HFE-7500, 3 M, supplemented with 2% wt/wt biocompatible surfactant) or PBS layer and then transferred into a count slide (Countess, Invitrogen) using a pipette. Droplet images were captured using a fluorescence microscope (EVOS, ThermoFisher).

Double emulsion droplets printing

The double emulsion droplet printer was obtained by integrating the double emulsion ejector with a droplet sorter. For double emulsion printing, the inner aqueous phase to generate inner cores was stained with FITC (green) or TRITC (red) at a final concentration of 100 μM, and the outer aqueous phase was stained with FITC at a final concentration of 2 μM as the background. The fluorescence signal was excited by a laser delivered through an inserted optical fiber (Thorlabs, Newton, NJ, with a cladding diameter of 225 μm, an optical core diameter of 200 μm, and an NA of 0.22) in the microfluidic chip with a wavelength of 473 nm. The emission signal was collected by the other optical fiber and detected by a PMT (Thorlabs, Newton, NJ), which was then utilized for control of the printing. The printing process was automated by a custom-made LabView interface. During printing, the substrate was placed on a XY mechanical stage (MA-2000, ASI, Eugene, OR) that was connected to a PC with a printer controller, and the sorting electrode was connected to a high voltage amplifier (690E-6, Trek, Lockport, NY) with a working voltage of ~ 2 kV. The ejected double emulsion droplets were deflected by a dielectrophoresis field into the vacuum collection tubing, and on-demand droplet printing was achieved by selectively sorting desired droplets for printing through reading the printing code in the software.

Data availability statement

The data that support the findings of this study are available from the corresponding author upon reasonable request.

Author contributions

P. Z. and A. R. A designed the research. P. Z. performed the experiments and analyzed the data. L. X. assisted with data analysis. P. Z. and A. R. A. wrote the manuscript with input from all authors.

Conflicts of interest

There are no conflicts to declare.

Acknowledgements

This work was supported by the National Science Fund for Distinguished Young Scholars (Overseas), the National Natural Science Foundation of China (Grant Number 52205296), the Chan Zuckerberg Biohub, and the National Institutes of Health (Grant Numbers 2R01EB019453 and 1DP2AR068129).

References

1 N. Garti, *Colloids Surf., A*, 1997, **123**, 233–246.
2 J. A. Hanson, C. B. Chang, S. M. Graves, Z. Li, T. G. Mason and T. J. Deming, *Nature*, 2008, **455**, 85–88.
3 S. Ding, C. A. Serra, T. F. Vandamme, W. Yu and N. Anton, *J. Controlled Release*, 2019, **295**, 31–49.

4 H. Lee, C. H. Choi, A. Abbaspourrad, C. Wesner, M. Caggioni, T. Zhu, S. Nawar and D. A. Weitz, *Adv. Mater.*, 2016, **28**, 8425–8430.
5 H. S. Jeong, E. Kim, C. Nam, Y. Choi, Y. J. Lee, D. A. Weitz, H. Lee and C. H. Choi, *Adv. Funct. Mater.*, 2021, **31**, 2009553.
6 Y. Y. Yang, T. S. Chung and N. P. Ng, *Biomaterials*, 2001, **22**, 231–241.
7 A. Edris and B. Bergnståhl, *Nahrung*, 2001, **45**, 133–137.
8 C. H. Chen, R. K. Shah, A. R. Abate and D. A. Weitz, *Langmuir*, 2009, **25**, 4320–4323.
9 C. X. Zhao, *Adv. Drug Delivery Rev.*, 2013, **65**, 1420–1446.
10 M. Iqbal, N. Zafar, H. Fessi and A. Elaissari, *Int. J. Pharm.*, 2015, **496**, 173–190.
11 W. Li, L. Zhang, X. Ge, B. Xu, W. Zhang, L. Qu, C.-H. Choi, J. Xu, A. Zhang, H. Lee and D. A. Weitz, *Chem. Soc. Rev.*, 2018, **47**, 5646–5683.
12 A. S. Utada, E. Lorenceau, D. R. Link, P. D. Kaplan, H. A. Stone and D. A. Weitz, *Science*, 2005, **308**, 537–541.
13 L. Y. Chu, A. S. Utada, R. K. Shah, J. W. Kim and D. A. Weitz, *Angew. Chem.*, 2007, **119**, 9128–9132.
14 Á. G. Marín, I. G. Loscertales, M. Marquez and A. Barrero, *Phys. Rev. Lett.*, 2007, **98**, 014502.
15 A. R. Abate and D. A. Weitz, *Small*, 2009, **5**, 2030–2032.
16 W. Wang, R. Xie, X. J. Ju, T. Luo, L. Liu, D. A. Weitz and L. Y. Chu, *Lab Chip*, 2011, **11**, 1587–1592.
17 P. E. Verboket, O. Borovinskaya, N. Meyer, D. Günther and P. S. Dittrich, *Anal. Chem.*, 2014, **86**, 6012–6018.
18 D. J. Sukovich, S. T. Lance and A. R. Abate, *Sci. Rep.*, 2017, **7**, 39385.
19 H. Fukaya and T. Uchimura, *Anal. Sci.*, 2017, **33**, 1067–1070.
20 K. K. Brower, M. Khariton, P. H. Suzuki, C. Still, G. Kim, S. G. Calhoun, L. S. Qi, B. Wang and P. M. Fordyce, *Anal. Chem.*, 2020, **92**, 13262–13270.
21 K. K. Brower, C. Carswell-Crumpton, S. Klemm, B. Cruz, G. Kim, S. G. Calhoun, L. Nichols and P. M. Fordyce, *Lab Chip*, 2020, **20**, 2062–2074.
22 H. J. Mea, L. Delgadillo and J. Wan, *Proc. Natl. Acad. Sci. U. S. A.*, 2020, **117**, 14790–14797.
23 A. M. Gañán-Calvo, *Phys. Rev. Lett.*, 1998, **80**, 285.
24 I. G. Loscertales, A. Barrero, I. Guerrero, R. Cortijo, M. Marquez and A. M. Ganan-Calvo, *Science*, 2002, **295**, 1695–1698.
25 D. Liu, B. Hakimi, M. Volny, J. Rolfs, X. Chen, F. Turecek and D. T. Chiu, *Anal. Chem.*, 2013, **85**, 6190–6194.
26 A. Evangelio, F. Campo-Cortés and J. M. Gordillo, *J. Fluid Mech.*, 2016, **804**, 550–577.
27 K. He, F. Campo-Cortés, M. Goral, T. López-León and J. M. Gordillo, *Phys. Rev. Fluids*, 2019, **4**, 124201.
28 H. Liu, J. A. Piper and M. Li, *Anal. Chem.*, 2021, **93**, 10955–10965.
29 S. C. Kim, D. J. Sukovich and A. R. Abate, *Lab Chip*, 2015, **15**, 3163–3169.
30 M. Pascual, M. Kerdraon, Q. Rezard, M. C. Jullien and L. Champougny, *Soft Matter*, 2019, **15**, 9253–9260.
31 Y. Jia, Y. Ren, L. Hou, W. Liu, X. Deng and H. Jiang, *Small*, 2017, **13**, 1702188.
32 F. Qu, S. Zhao, G. Cheng, H. Rahman, Q. Xiao, R. W. Y. Chan and Y. P. Ho, *Microsyst. Nanoeng.*, 2021, **7**, 38.
33 L. Chen, Y. Xiao, Q. Wu, X. Yan, P. Zhao, J. Ruan, J. Shan, D. Chen, D. A. Weitz and F. Ye, *Small*, 2021, **17**, 2102579.
34 P. Zhang and A. R. Abate, *Adv. Mater.*, 2020, **32**, 2005346.